



Technical note

Effect of screw thread length on stiffness of proximal humerus locking plate constructs: A finite element study

Louise Le^{a,†}, Ali Jabran^{a,†}, Chris Peach^{a,b}, Lei Ren^{a,*}^a School of Mechanical, Aerospace and Civil Engineering, University of Manchester, Manchester, M13 9PL, United Kingdom^b Department of Shoulder and Elbow Surgery, University Hospital of South Manchester, Manchester, United Kingdom

ARTICLE INFO

Article history:

Received 13 March 2018

Revised 3 November 2018

Accepted 4 December 2018

Keywords:

Proximal humerus plates

Finite element analysis

Screw Threading

Varus Bending

Stiffness

ABSTRACT

Plate-based treatment of proximal humerus fractures is associated with a high risk of complications such as screw perforation into glenohumeral joint. Smooth and threaded pegs were developed with the hope of minimising these risks. No consensus exists onto which threading profile achieves stiffest bone-plate construct. This study investigated the biomechanical effect of five percentages of threading on individual humeral head screws on a bone-plate construct. A finite element model simulating a two-part proximal humerus fracture treated with a Spatial Subchondral Support plate was developed and validated against in vitro biomechanical tests. The proportion of the humeral head screw length that was threaded was varied between 0%–100% in 25% increments. A 5-mm cantilever varus displacement was applied and the required load (F_5) was calculated. Full (100%) threading achieved the stiffest construct for all six screws. Fully threading all smooth pegs at once increased F_5 by 18%. Threading did not increase F_5 equally in all screws. Inferior three plate screws exhibited a larger increase in stiffness than superior three. Most of the mechanical benefits of threading in inferior three screws can be achieved by using threaded pegs (50% threading) while the superior three screws need to be fully threaded. In practice, the smooth surface profile may also offer additional mechanical benefits if implanted with longer lengths and larger diameters. Threading is an effective way of increasing the varus bending stiffness of proximal humerus plates constructs.

© 2018 IPPEM. Published by Elsevier Ltd. All rights reserved.

1. Background

Proximal humerus fractures account for 5% of all fracture types and 10% of fractures in the over-65 patient population [1,2]. While they can be treated non-operatively, their operative treatment modalities include intramedullary nails, percutaneous fixation and open reduction internal fixation with locking plates. The latter exhibits superior in vitro biomechanical performance than earlier fixation methods [3–10]. In clinical practice, these plates are associated with issues such as screw glenohumeral perforation which have a complication rate of up to 23% [11–17].

Several factors can increase the risk of primary screw perforation. Locking screws can feel tight during insertion because of the locking mechanism and their true purchase in the bone cannot be felt, creating a deceptive sense of security [18]. Insertion of diverging and converging screws into the spherical humeral head surface can make it difficult to correctly assess their tip position on orthogonal views [19,20]. Further, the limited tactile feedback

provide by the drill bit feedback can cause over-drilling of the poor-quality, osteoporotic bone. Secondary screw perforation can occur if the resulting longer screw holes are left unnoticed during surgery and even after minimising these technical errors [17,19,20]. Screws of locking plates cannot back out during humeral head collapse and instead perforate into the joint [21]. If left untreated, glenoid surface can erode extensively, necessitating hemiarthroplasty or total shoulder arthroplasty as a salvage procedure. Using non-locking screws may prevent this but at the cost of mechanical stability of bone-plate construct and at risk of disengagement of screws from plate [21].

Screws of locking plates structurally support the humeral head, preventing its collapse by resisting the bending moments experienced during bone loading. During cantilever bending, their bending strength is cubically proportional to their core diameter [22,23]. Bone-screw interface is crucial to enhance their purchase and the pull-out strength [24–28]. Orientating them toward high bone quality regions (e.g. subchondral region) can improve their purchase [29]. Pull-out resistance depends on the bone volume between their threads and therefore their length and surface profile (thread's pitch, depth and geometry) [22,23]. Screws must also prevent articular damage, particularly after humeral head collapse.

* Corresponding author.

E-mail address: lei.ren@manchester.ac.uk (L. Ren).

† Equal contribution.

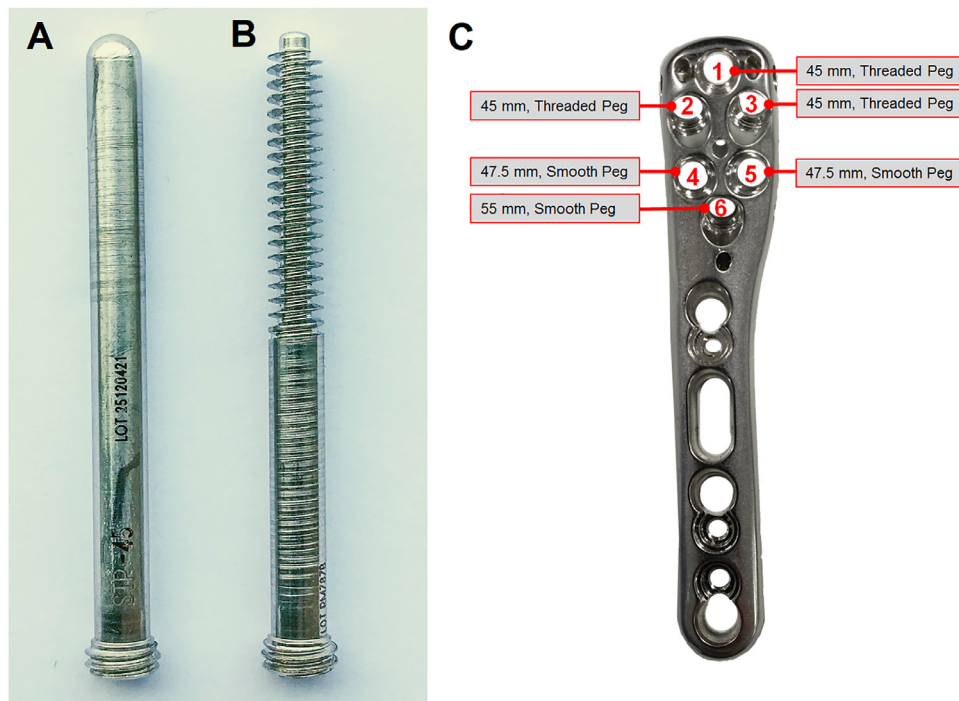


Fig. 1. Smooth (A) and threaded (B) pegs fixation options provided by the S3 plate and (C) the number, lengths and profile description of the humeral head screws used in the initial FE model.

Several millimetres of clearance is kept between screw tip and articular surface [30]. However, this can reduce their contact with subchondral bone.

Spatial Subchondral Support (S3) proximal humerus plate (Zimmer Biomet, IN, USA) aims to prevent articular surface damage by modifying the screw surface profile. While most proximal humerus plates have threaded screws, S3 plate also offers smooth pegs and threaded pegs (Fig. 1). Badman et al. likened the smooth pegs' structural support to humeral head to that of rebar in concrete [31]. These blunt-tipped smooth pegs are believed to cause less glenohumeral damage than threaded screws [31,32] and can be kept longer to attain subchondral abutment. Although their bone purchase is not as direct as threaded screws, their smooth profile allows for greater core diameters, providing the required bending strength. Threaded pegs combine the smooth surface and large diameter of pegs with direct bone purchase of threads (Fig. 1B).

No general consensus exists in the clinical and in vitro biomechanical testing literature onto what percentage of threading achieves stiffest construct and whether this percentage is same for all plate screws [32–38]. Also, with the lack of in silico mechanical studies on this, the choice of screw type is currently left to the clinician's discretion based on their experiences.

The objective of this finite element (FE) study is two-folded. Firstly, we will compare the varus bending stiffness of a proximally fractured humerus treated with an S3 plate with all head screws fully threaded to that with all head screws smoothed (smooth pegs). Secondly, we will systemically examine the effect of threading percentage of each head screw on the bending stiffness of the bone-plate construct.

2. Material and methods

2.1. Pseudo-threading in a cylindrical bone model

An FE model of a cylindrical bone and a screw was developed and validated using the pseudo-threading technique of modelling the bone-screw interface described by Inzana et al. [39]. A locking

screw was modelled in Solid Edge (Siemens PLM Software TX, USA) as cylinders (3.5 mm head diameter, 2.96 mm core diameter). Two helices with (pitch: 0.85 mm, helical offset: 0.35 mm) were drawn on screw shaft. Helical ends were connected to create a helical surface representing the pseudo-threaded region (Fig. 2A). Screw was inserted 12 mm deep into a 20-mm diameter hole located in a 15-mm long cylinder representing the bone (Fig. 2B).

Screw and bone were imported into Abaqus CAE Standard 6.13 (Dassault Systemes, Simulia Corp, Providence, RI, USA) and respectively modelled with material properties of titanium alloy (Young's modulus: 105 GPa, Poisson's ratio: 0.3) and bone (Young's modulus: 600 MPa, Poisson's ratio: 0.3) [39].

Uncoupled cohesive behaviour (K_{nn} : 0, K_{ss} : 10,000 N, K_{tt} : 0) was applied to the pseudo-threaded screw region and friction using the penalty method (friction coefficient: 0.3, maximum elastic slip = 0.005) was applied on surfaces between pseudo-threads. A reference point was created 1.5 mm above the top surface's centre and constrained to this surface via kinematic coupling. A 50 N concentrated force was applied to the reference point at a 45° angle increment between 0° (axial pulling) and 180° (Fig. 2B). Pinned boundary conditions were applied to cylindrical bone's curved and bottom surface. All parts were meshed using quadrilateral tetrahedral elements (C3D10), leading to a total node count of 50,526, similar to Inzana et al. (52,217). Absolute principal strain distributions were qualitatively validated against distributions from Inzana et al. [39].

2.2. Bone-plate finite element model with pseudo-threading

Once validated, this pseudo-threading technique was implemented in an FE model simulating varus bending of a proximally fractured humerus treated with an S3 plate. CT scan dataset of a synthetic left humerus (model 1028; Pacific Research Laboratories, Vashon, WA, USA) was acquired using SOMATOM CT Scanner (SOMATOM, Siemens, Munich, Germany) and segmented in Mimics 16.0 software (Materialise, Leuven, Belgium) to develop the surface model of the humerus. Two-part surgical neck fracture was

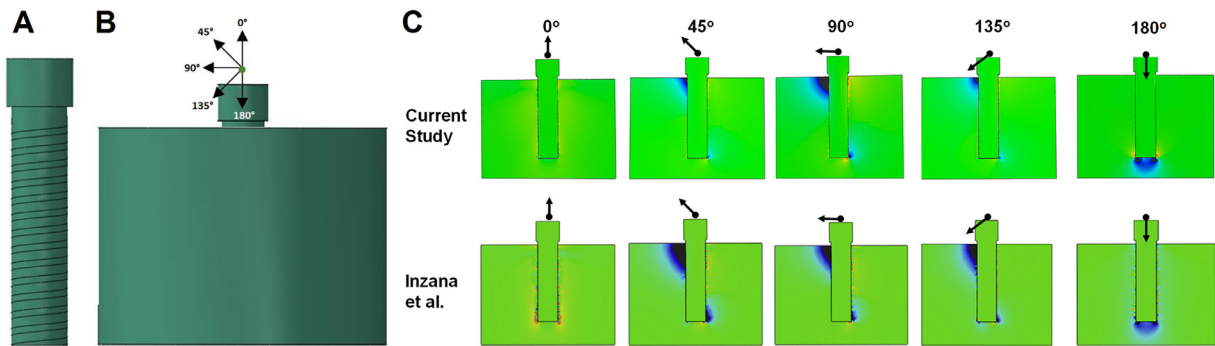


Fig. 2. A pseudo-threaded screw (A) inserted into a cylinder bone with load applied at an angle of 0°, 45°, 90°, 135° and 180° (B) and the absolute principal strain distributions obtained in this study compared to those reported by Inzana et al. [39].

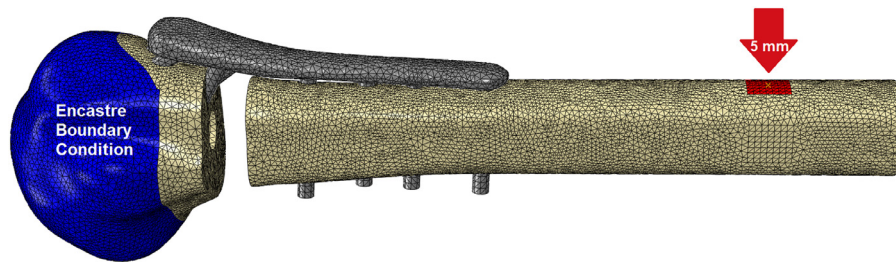


Fig. 3. Assembly of humerus and S3 plate in the FE model and selection of the head surface to apply encastre boundary condition (blue) and the shaft surface to apply varus displacement (red).

Table 1

Material and mesh properties of the plate and the humeral head and shaft.

	Young's modulus (MPa)	Poisson's ratio	Element count
Humeral head	257.78	0.3	276,998
Humeral shaft	257.78	0.3	205,104
S3 plate	193,000	0.3	35,832

simulated by removing a 10 mm bone section, 50–60 mm from humeral head apex. Further, bone located more than 210 mm away from the head apex was removed. Surface model of an 83 mm long S3 plate was developed using a FaroArm 3D laser scanner (Faro Technologies, Lake Mary, FL, USA).

Plate and bone surface models were converted into solid models using Geomagic Wrap 2014 software (3D Systems, Rock Hill, SC, USA) and imported into Solid Edge. Screws were modelled as cylinders and merged with plate [40,41]. For pseudo-threading, two helices were drawn on screws' surface (pitch: 1.0 mm, helical offset: 0.46 mm). Helical ends were connected to create a helical surface representing the threads. Screws 1–3 were pseudo-threaded along half their lengths to represent threaded pegs and screws 4–6 were left smooth to represent smooth pegs (Fig. 1C).

Humeral head, shaft and plate models were imported into Abaqus as 3D deformable parts. Their assembly and material properties (linear elastic, isotropic) were based on manufacturers' specification (Table 1) [42–44]. Cohesive behaviour and frictional settings on threaded pegs were same as that for cylindrical bone FE model. Only friction was applied to smooth pegs whereas shaft screws were fully threaded and had tie constraints.

Encastre boundary condition was applied to all humeral head surfaces located less than 40 mm from the humeral head apex, restricting all displacements and rotations there (Fig. 3). A 100 mm² square surface was created on the humeral shaft, with its centre 180 mm away from the head apex. A reference point was created above this surface, coupled to it and displaced 5 mm along the varus direction to induce varus bending of bone-plate construct. Varus bending was applied since humeral head varus collapse is

one of the main complications associated with proximal humerus plates, often leading to secondary screw perforation [21,26]. All parts were meshed using 10-node quadratic tetrahedron (C3D10) elements (global seed size: 1.5, local seed size: at 1.0), resulting in an element count of 517,934 for assembly. The simulation time was approximately 52 h on a 20 GB RAM computer with 5 processing cores. To represent the construct's varus bending stiffness, the load required to apply 5 mm displacement (F_5) was recorded.

A convergence test was conducted to determine the optimum mesh seed size and the final element count. FE models with 152,914 to 2,045,170 elements were analysed, all with bone-screw interface tied. They converged successfully as their bending forces (F_5) differed by only 0.33%. Simulation time ranged from 20 min to 7 days on a computer with 5 processing cores and 20 GB RAM. Medium mesh density was selected due to its relatively short simulation time (~3 h) and fine mesh.

For FE model validation, in vitro biomechanical tests were conducted on five synthetic humeri that were identical to that used in the FE model [45]. A 10 mm surgical neck fracture was simulated on all specimens and their distal ends were cut 210 mm below humeral head apex. S3 plate with same screw lengths and types as the FE model were implanted. Humeral head was potted 40 mm into a custom-made cubic cement block to restrict its displacements and rotations. With the block clamped, a universal testing machine (Instron 4500, Canton, MA, USA) perpendicularly displaced the humeral shaft for 5 mm in the varus direction at 5 mm/s displacement, at a point 180 mm from the head apex. This cantilever bending was performed five times for each specimen and the load-displacement data was used to determine experimental load (F_5).

2.3. Bone-plate finite element analysis with different threading percentages

This model was used to develop 26 FE models: one with all six head screws smooth, one with all six head screws fully threaded and twenty-four with 25%, 50%, 75% and 100% threading of the six

Table 2

Load required to apply 5 mm varus displacement (F_5) for 0%, 25%, 50%, 75% and 100% threading of all six screws.

Threading (%)	Screw 1	Screw 2	Screw 3	Screw 4	Screw 5	Screw 6
0	51.8624	51.8624	51.8624	51.8624	51.8624	51.8624
25	51.8740	51.9706	52.1004	53.6872	53.7185	52.7146
50	51.9041	51.9973	52.2259	54.0003	53.8825	52.9749
75	52.0275	52.0539	52.3581	54.1018	53.9291	53.0351
100	52.2372	52.1179	52.3623	54.2199	53.9636	53.0759

Table 3

Percentage change in the load required to apply 5 mm varus displacement (F_5) for 25%, 50%, 75% and 100% threading of all six screws in comparison with the model with all screws smooth.

Threading (%)	Screw 1	Screw 2	Screw 3	Screw 4	Screw 5	Screw 6
25	0.0224	0.2086	0.4589	3.5185	3.5789	1.6432
50	0.0804	0.2601	0.7009	4.1223	3.8951	2.1451
75	0.3183	0.3692	0.9558	4.3180	3.9850	2.2612
100	0.7227	0.4926	0.9639	4.5457	4.0515	2.3398

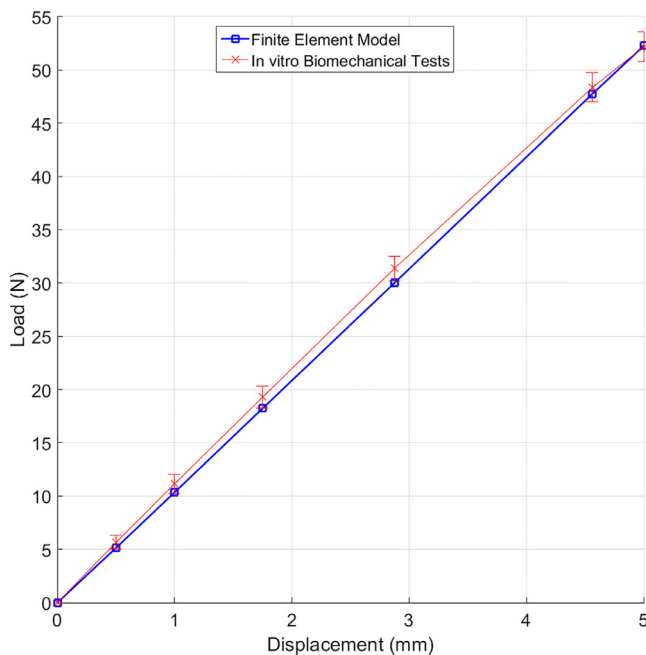


Fig. 4. Load–displacement relationship predicted by the FE model compared with the in vitro biomechanical measurement data (mean \pm S.D.).

head screws. The remaining preparation process was identical to that in the preceding section.

3. Results

Absolute principal strain distributions of the simple cylindrical bone model were qualitatively similar to Inzana et al., especially the strain magnitude and location for 45°, 90°, 135° and 180° loading (Fig. 2C). This validated the pseudo-threading technique. FE model of the S3 plate construct predicted similar F_5 values (only 0.178% higher) to those recorded in vitro. Because of this and the good agreement in their load-displacement curves, the FE model was considered validated (Fig. 4).

The fully-threaded plate had 18% greater F_5 (61.4215 N) than fully-smooth plate (51.8624 N). Increasing percentage threading of any screw increased F_5 (Fig. 5A,B and Tables 2 and 3). Full thread-

ing did not affect all screws equally. It increased F_5 by 4.55% in screw 4 but only 0.49% in screw 2. In general, the lower three screws (4, 5 and 6), particularly the inferomedial screws (4 and 5) were more sensitive to threading than the upper three. For screws 2–6, increasing threading from 0%–50% increased F_5 more than from 75%–100%, even after normalising for screw length (Fig. 5C and Table 4). Screws 4–6 had to be 50% threaded, screw 3, 75% threaded, and screws 1 and 2, 100% to achieve 90% of their maximum F_5 value (Table 5).

Threading the head screws by any amount increased the mean von Mises stress in their respective screw holes (Table 6). With the exception of screw 4, this increase was incremental as percentage threading was increased.

Fully-threading all head screws increased the mean von Mises stress in head screws holes (39.26%–121.69%) more than in shaft screws holes (18.49%–18.59%). It reduced mean von Mises stresses on surfaces of head screws by 34.48%–42.10% but increased on surfaces of shaft screws by 17.44%–21.75% (Table 7). There was no clear relationship between percentage threading of a screw and the mean von Mises stress on other screws' surfaces.

Irrespective of percentage threading, mean von Mises stress on screw 10's hole was higher than that on all other screw holes. Generally, the mean von Mises stresses on surfaces of screws 2 and 3 were noticeably the highest while those on screws 8 and 9 were often the lowest among the screws.

4. Discussion

As for the first aim of this study, fully-threaded constructs were stiffer than smooth peg constructs during varus bending. The in vitro studies on distal radius plates report their superiority during axial compression [34,36] and torsion [34,35]. Their clinical stability and in vitro axial stiffness are reportedly similar [35,37,38]. As for proximal humerus fractures, Schumer et al. [32] found no statistically significant difference between S3 plate's threaded pegs and smooth pegs during axial compression and torsion. Only one study reported stiffer constructs with the use of smooth pegs in place of threaded screws, albeit only during varus bending and not during torsion [33]. However, it was difficult to distinguish whether this stiffness difference was due to screw profile, screw length or plate geometry.

The second aim of this study was to examine the effect of screw threading on construct stiffness. In all head screws, construct stiffness increased with increasing threading percentage albeit by dif-

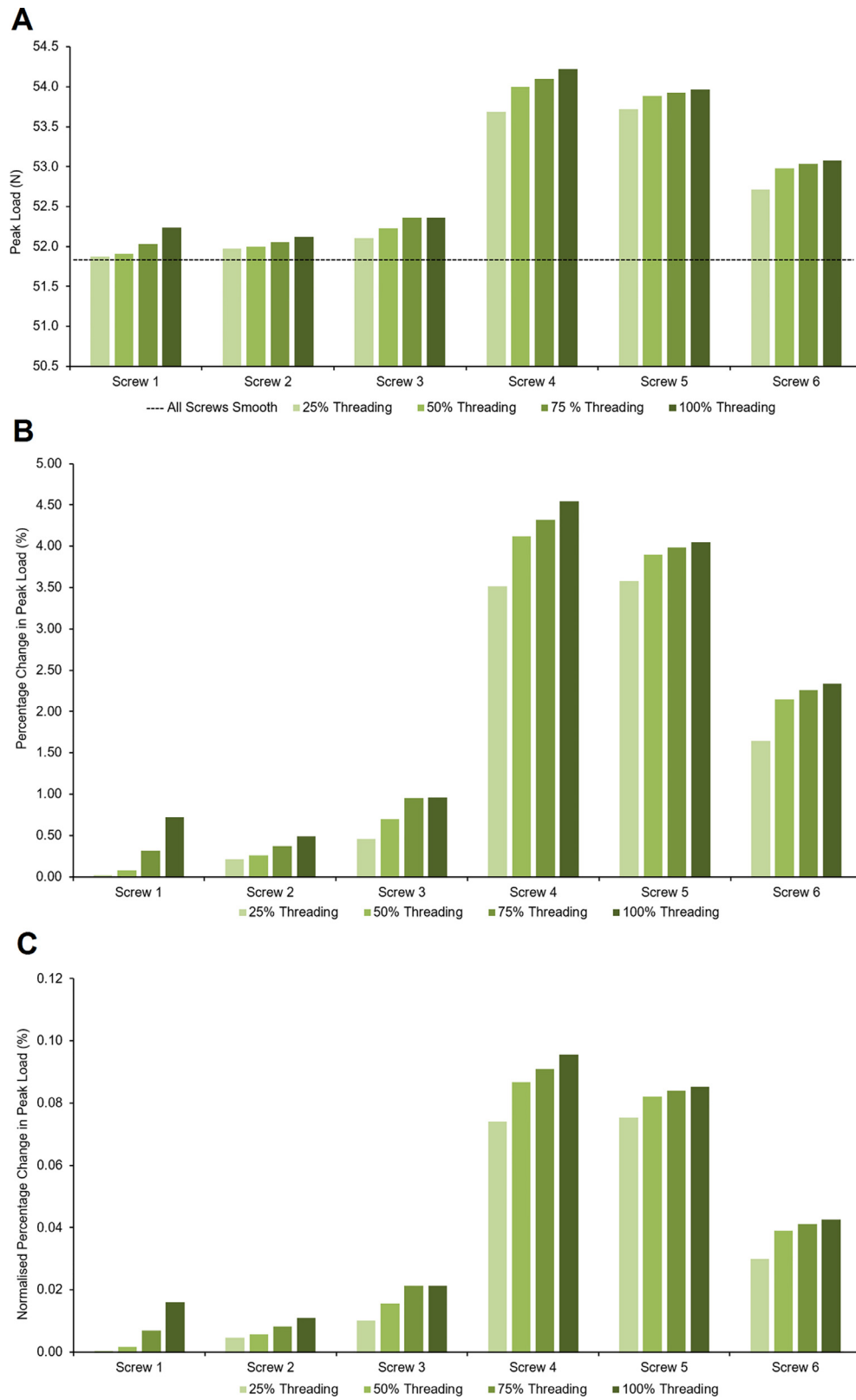


Fig. 5. (A) F_5 , (B) percentage change in F_5 and (C) screw length-normalised percentage change in F_5 for 25%, 50%, 75% and 100% threading of each of the six head screws in comparison with the F_5 value when all screws were smooth pegs. Dashed line represents F_5 of this smooth peg construct.

Table 4

Percentage change in the load required to apply 5 mm varus displacement (F_5) for 25%, 50%, 75% and 100% threading of all six screws in comparison with the model with all screws smooth and normalised by screws' lengths.

Threading (%)	Screw 1	Screw 2	Screw 3	Screw 4	Screw 5	Screw 6
25	0.000	0.005	0.010	0.074	0.075	0.030
50	0.002	0.006	0.016	0.087	0.082	0.039
75	0.007	0.008	0.021	0.091	0.084	0.041
100	0.016	0.011	0.021	0.096	0.085	0.043

Table 5

Cumulated percentage change in the load required to apply 5 mm varus displacement (F_5) for each 25% increment in threading of all six screws.

	Screw 1	Screw 2	Screw 3	Screw 4	Screw 5	Screw 6
0%	0.000	0.000	0.000	0.000	0.000	0.000
25%	3.099	42.347	47.609	77.403	88.335	70.228
50%	11.125	52.801	72.715	90.686	96.140	91.679
75%	44.043	74.949	99.160	94.991	98.359	96.641
100%	100.000	100.000	100.000	100.000	100.000	100.000

Table 6

Effect of percentage threading on the mean von Mises stress (MPa) of each screw hole (bony surface).

Screw	Threading	Screw Hole									
		1	2	3	4	5	6	7	8	9	10
1-6	0%	0.599	0.699	0.680	0.627	0.613	0.539	0.930	0.662	0.721	2.499
	25%	0.628	0.696	0.678	0.627	0.613	0.535	0.930	0.662	0.721	2.500
	50%	0.695	0.693	0.671	0.627	0.614	0.537	0.931	0.663	0.721	2.501
	75%	0.852	0.681	0.655	0.624	0.617	0.539	0.933	0.664	0.723	2.507
	100%	0.869	0.655	0.623	0.617	0.618	0.533	0.937	0.667	0.726	2.517
1	25%	0.554	0.861	0.641	0.620	0.619	0.543	0.933	0.666	0.724	2.511
	50%	0.535	0.992	0.627	0.617	0.623	0.545	0.936	0.667	0.726	2.516
	75%	0.520	1.004	0.617	0.608	0.625	0.543	0.939	0.669	0.728	2.523
	100%	0.516	1.022	0.615	0.604	0.624	0.539	0.939	0.669	0.728	2.523
2	25%	0.578	0.681	0.786	0.626	0.615	0.541	0.931	0.664	0.723	2.504
	50%	0.579	0.679	0.857	0.626	0.617	0.541	0.932	0.664	0.723	2.505
	75%	0.573	0.671	0.896	0.626	0.617	0.542	0.933	0.665	0.724	2.508
	100%	0.564	0.666	0.912	0.625	0.609	0.535	0.934	0.666	0.725	2.511
3	25%	0.711	0.615	0.693	1.126	0.555	0.461	0.963	0.686	0.747	2.589
	50%	0.723	0.606	0.696	1.174	0.561	0.448	0.966	0.688	0.749	2.597
	75%	0.720	0.601	0.695	1.232	0.560	0.438	0.966	0.689	0.750	2.599
	100%	0.489	0.416	0.476	0.884	0.388	0.294	0.669	0.477	0.518	1.797
4	25%	0.686	0.658	0.654	0.590	1.097	0.451	0.963	0.686	0.746	2.587
	50%	0.701	0.651	0.651	0.591	1.249	0.428	0.968	0.690	0.751	2.602
	75%	0.699	0.647	0.647	0.592	1.309	0.422	0.970	0.691	0.752	2.607
	100%	0.693	0.644	0.644	0.600	1.355	0.428	0.969	0.690	0.751	2.604
5	25%	0.708	0.695	0.718	0.616	0.582	0.885	0.945	0.673	0.733	2.540
	50%	0.735	0.678	0.705	0.629	0.597	0.953	0.949	0.677	0.736	2.553
	75%	0.730	0.667	0.688	0.623	0.614	1.015	0.950	0.678	0.737	2.556
	100%	0.721	0.666	0.682	0.629	0.635	1.057	0.952	0.678	0.738	2.558
6	25%	1.071	1.276	0.947	1.390	1.237	0.863	1.102	0.785	0.855	2.961
	50%										
	75%										
	100%										
1-6	100%	1.071	1.276	0.947	1.390	1.237	0.863	1.102	0.785	0.855	2.961

Table 7
Effect of percentage threading on the mean von Mises stress (MPa) of each screw's surface.

Screw	Threading	Screw									
		1	2	3	4	5	6	7	8	9	10
1-6	0%	47.459	54.768	54.501	48.129	48.465	47.259	33.062	8.750	4.739	32.973
	25%	34.846	54.110	54.248	47.786	48.409	46.798	32.943	8.831	4.752	33.287
	50%	32.860	54.382	54.346	47.197	48.639	46.875	32.937	8.978	4.728	33.636
	75%	40.054	54.128	53.818	47.624	48.102	46.518	33.598	8.871	4.764	33.241
	100%	50.314	52.898	52.991	47.563	48.220	45.842	33.491	8.948	4.844	33.497
2	25%	46.910	37.442	53.142	47.710	48.715	46.299	33.148	9.030	4.817	33.327
	50%	47.643	37.991	53.009	47.319	48.175	46.024	32.965	9.013	4.787	33.726
	75%	47.102	48.345	52.720	47.351	48.100	45.758	33.129	9.099	4.802	33.947
	100%	47.035	54.858	52.588	47.361	48.544	45.972	33.360	9.117	4.804	32.985
3	25%	47.906	54.007	39.117	47.611	48.873	46.579	33.482	8.979	4.875	34.050
	50%	47.545	53.985	37.693	47.665	48.673	46.623	33.059	8.896	4.774	32.708
	75%	47.639	53.742	46.617	47.425	48.257	46.122	33.723	9.016	4.796	32.843
	100%	46.863	53.879	54.989	47.243	48.458	46.237	33.411	8.991	4.716	33.107
4	25%	45.267	52.938	51.125	36.106	45.032	44.703	34.102	9.246	4.978	34.320
	50%	45.723	52.224	51.608	37.130	44.821	44.570	34.552	9.292	5.022	34.632
	75%	45.685	52.063	51.091	44.469	44.647	44.674	34.577	9.299	4.900	34.793
	100%	31.254	35.986	35.462	33.048	30.861	30.836	23.795	6.421	3.453	23.338
5	25%	45.392	51.427	51.201	44.191	35.722	44.418	33.589	9.189	4.918	34.463
	50%	44.610	50.984	51.343	43.497	35.894	44.165	34.315	9.361	4.947	34.681
	75%	44.729	50.910	51.221	42.618	43.298	44.026	34.781	9.289	5.061	34.462
	100%	45.057	50.599	50.627	43.025	47.418	44.398	34.561	9.358	5.039	33.901
6	25%	47.069	53.215	52.537	45.614	46.890	34.791	33.992	9.011	4.888	33.604
	50%	46.763	52.801	52.894	45.175	45.882	37.131	33.540	9.161	4.926	33.906
	75%	46.359	53.381	52.623	44.849	45.682	44.825	33.637	9.188	4.935	34.203
	100%	45.790	53.682	52.146	44.906	45.898	46.492	33.522	9.210	4.876	33.815
1-6	100%	29.260	31.708	32.212	31.532	31.667	29.302	38.827	10.653	5.738	39.379

ferent amounts. Fully threading the inferomedial screws (4 and 5) increased F_5 by 4.55%, nine times more than that by fully threading screw 2 (0.49%). Threading affected the lower three screws (4–6) more than the upper three where the percentage increase in F_5 due to full threading of screws 4 (4.55%), 5 (4.05%) or 6 (2.34%) was more than the combined total increase by screws 1–3 (2.18%). This cannot be solely attributable to the lower screws' proximity to the fracture site, otherwise, threading screw 6 would have had a more significant impact on stiffness than either screws 4 or 5. This may be because screws 4 and 5 are divergent and directed towards the inferomedial region of the humerus, a region critical for humeral head's stability against varus collapse [25,28]. To achieve 90% of their respective maximum F_5 values, screws 4–6 must be threaded 50%, screw 3 must be 75% threaded and screws 1 and 2 must be fully threaded. Since 75% threading is commercially unavailable, we recommend fully threading the upper three screws and using threaded pegs in the lower three.

Overall, threading decreased the mean von Mises stress on the head screws' surfaces but increase it in their screw hole surfaces. Thus, a compromise between screw hole surface stress and F_5 is needed to determine the ideal percentage of threading. A clear relationship was not found between the incremental increase in the percentage threading (e.g. from 25% to 50%) of a screw and the mean von Mises stresses on the surfaces of the other nine screws. Furthermore, the bias between the effect of threading the inferior and the superior screws was not reported, with the exception of full threading of screw 4 which led to a relatively large reduction

in the mean von Mises stress in each screw's surface. A wide range of factors including the geometry and the material properties of bone surrounding the screw and the position and orientation of a screw with respect to other screws may have contributed to this complex relationship between percentage threading and mean von Mises stress.

In this study, pseudo-threading technique was successfully implemented on proximal humerus plates. FE studies on proximal humerus plates in the literature are limited by the bone–screw interface, which is idealised either by perfectly bonding the bone–screw interfacial surfaces or having frictional contacts, typically applied to the entire screw shaft surface [40,46–48]. Screw threads interact differently with bone than unthreaded areas and have different local peak strains. Analyses of screws modelled this way are less sensitive than if interactions were applied to specific regions of the screw.

For accurate loads and stress distribution results, screw surface must be modelled as realistic as possible. Explicitly modelling the screw thread geometry is computationally expensive and difficult to mesh. Inzana et al. approximated screws as smooth cylinders with the threads implicitly represented through interfacial surface interactions, i.e. pseudo-threaded screws instead of perfectly bonded connections or true screw geometry with friction. During their pull-out tests, pseudo-threaded modelling obtained more accurate screw displacements, strain distribution and strain magnitudes of the explicitly threaded model than the smooth cylinder with tie constraint.

Unlike in vitro and in vivo testing, in silico methods (e.g. FE method) allow easy changes to individual parameters in isolation. To minimise the influence of local material properties on mechanical performance that is commonly experienced in cadaveric studies, we used synthetic humeri during in vitro tests. In the FE model, we merged the cortical and cancellous bone regions and modelled them with homogenous material properties. More accurate modelling of the bone density distribution of these regions may accentuate the effects of threading, especially for threading increments (e.g. 25%) abutting the high-density subchondral region [30,36]. Due to pseudo-threading technique's insensitivity to Young's modulus of bone [39], such a model can involve bones with a range of material properties.

All loads in this study were static whereas cyclic loading is required for fatigue analysis, which may accentuate the mechanical differences among specimens. For example, static in vitro testing by Mehling et al. showed statistically similar axial and torsional stiffness with the use of threaded pegs and smooth pegs [34]. By adding a cyclic torsion step, there difference became statistically significant. Threaded screw constructs had higher median axial and torsional stiffness than smooth peg constructs. One possible explanation is that the peg's smooth surface forms a less stable interface with bone than threads. Although insignificant during static testing, pegs slide along the screw hole with progression of cyclic loading whereas the threads restrict its movement. Yamamoto et al. noted this, reporting that the difference in fragment displacements of smooth- and threaded-peg constructs became more apparent as the cyclic bending test progressed [33]. Schumer et al., however, reported no statistically significant difference between smooth pegs and threaded pegs during both static and cyclic loading [32]. However, factors such as the implant choice, fracture type and load magnitude may have influenced this.

To isolate the effects of threading, lengths and diameters of all screws were kept constant. Normalising the F_5 loads by screw length did not affect the trends in F_5 values. However, if the bone density distribution is modelled more accurately, the structural advantage of longer screws, especially those abutting the subchondral region, is likely to be more pronounced. Similarly, threaded and unthreaded screw regions had the same diameter, whereas, in reality, unthreaded regions have larger diameters and provide more mechanical support. Considering these factors, smooth pegs may have additional mechanical advantages over fully-threaded screws in the clinic.

5. Conclusion

We tested bone-plate construct in a pre-collapse scenario, where the plate was in good contact with the fracture fragments. Here the role of the screws was to provide the mechanical support necessary to maintain the head structure. Threading was an effective way of increasing the varus bending stiffness of proximal humerus plates constructs. Out of all threading percentages tested, full threading achieved the stiffest constructs, more than the threaded pegs. While threading increased construct stiffness in all six head screws of the S3 plate, it did not increase them equally. The three inferiorly located plate screws exhibited a larger increase in stiffness and most of the mechanical benefits of threading can be achieved by using threaded pegs. For the superior three screws, however, full threading is required to achieve the construct stiffness.

Smooth surface profile may offer additional mechanical benefits than those demonstrated in this study since they can usually be implanted with longer lengths and larger diameters than their threaded counterparts. Determining the risk of a screw's glenohumeral perforation necessitates an investigation of its role in preventing articular surface damage.

Acknowledgements

Competing interests

None declared.

Funding

This research was partly supported by the projects of UK Engineering and Physical Science Research Council (EP/K019759/1 and EP/I033602/1).

Ethical approval

Not required.

References

- [1] Baron JA, Karagas M, Barrett J, Kniffin W, Malenka D, Mayor M, et al. Basic epidemiology of fractures of the upper and lower limb among Americans over 65 years of age. *Epidemiology* 1996;7:612–18. doi:10.1097/00001648-199611000-00008.
- [2] Court-Brown CM, Caesar B. Epidemiology of adult fractures: a review. *Injury* 2006;37:691–7. doi:10.1016/j.injury.2006.04.130.
- [3] Chudik SC, Weinhold P, Dahners LE. Fixed-angle plate fixation in simulated fractures of the proximal humerus: a biomechanical study of a new device. *J Shoulder Elb Surg* 2003;12:578–88. doi:10.1016/S1058-2746(03)00217-9.
- [4] Clavert P, Adam P, Bevort A, Bonnomet F, Kempf JF. Pitfalls and complications with locking plate for proximal humerus fracture. *J Shoulder Elb Surg* 2010;19:489–94. doi:10.1016/j.jse.2009.09.005.
- [5] Duralde XA, Leddy LR. The results of ORIF of displaced unstable proximal humeral fractures using a locking plate. *J Shoulder Elb Surg* 2010;19:480–8. doi:10.1016/j.jse.2009.08.008.
- [6] Kitson J, Booth G, Day R. A biomechanical comparison of locking plate and locking nail implants used for fractures of the proximal humerus. *J Shoulder Elb Surg* 2007;16:362–6. doi:10.1016/j.jse.2006.01.019.
- [7] Siffri PC, Peindl RD, Coley ER, Norton J, Connor PM, Kellam JE. Biomechanical analysis of blade plate versus locking plate fixation for a proximal humerus fracture: comparison using cadaveric and synthetic humerus. *J Orthop Trauma* 2006;20:547–54. doi:10.1097/01.bot.0000244997.52751.58.
- [8] Ricchetti ET, Warrender WJ, Abboud JA. Use of locking plates in the treatment of proximal humerus fractures. *J Shoulder Elbow Surg* 2010;19:66–75. doi:10.1016/j.jse.2010.01.001.
- [9] Seide K, Triebe J, Faschingbauer M, Schulz AP, Püschel K, Mehrrens G, et al. Locked vs. unlocked plate osteosynthesis of the proximal humerus - a biomechanical study. *Clin Biomech* 2007;22:176–82. doi:10.1016/j.clinbiomech.2006.08.009.
- [10] Walsh S, Reindl R, Harvey E, Berry G, Beckman L, Steffen T. Biomechanical comparison of a unique locking plate versus a standard plate for internal fixation of proximal humerus fractures in a cadaveric model. *Clin Biomech* 2006;21:1027–31. doi:10.1016/j.clinbiomech.2006.06.005.
- [11] Charalambous CP, Siddique I, Valluripalli K, Kovacevic M, Panose P, Srinivasan M, et al. Proximal humeral internal locking system (PHILOS) for the treatment of proximal humeral fractures. *Arch Orthop Trauma Surg* 2007;127:205–10. doi:10.1007/s00402-006-0256-9.
- [12] Egol KA, Ong CC, Walsh M, Jazrawi LM, Tejwani NC, Zuckerman JD. Early complications in proximal humerus fractures (OTA Types 11) treated with locked plates. *J Orthop Trauma* 2008;22:159–64. doi:10.1097/BOT.0b013e318169ef2a.
- [13] Fankhauser F, Boldin C, Schippinger G, Haunschmid C, Szyzkowitz R. A new locking plate for unstable fractures of the proximal humerus. *Clin Orthop Relat Res* 2005;176–81. doi:10.1097/01.blo.0000137554.91189.a9.
- [14] Koukakis A, Apostolou CD, Taneja T, Korres DS, Amini A. Fixation of proximal humerus fractures using the PHILOS plate: early experience. *Clin Orthop Relat Res* 2006;442:115–20.
- [15] Owsley KC, Gorczyca JT. Displacement/screw cutout after open reduction and locked plate fixation of humeral fractures. *J Bone Jt Surg* 2008;90:223–40. doi:10.2106/JBJS.E.01351.
- [16] Aaron D, Shatsky J, Paredes JC, Parsons BO, Flatow EL. Proximal humeral fractures: internal fixation. *J Bone Jt Surg Ser A* 2013;94:2279–88.
- [17] Sproul RC, Iyengar JJ, Devic Z, Feeley BT. A systematic review of locking plate fixation of proximal humerus fractures. *Inj J Care Inj* 2011;42:408–13. doi:10.1016/j.injury.2010.11.058.
- [18] Smith WR, Ziran BH, Anglen JO, Stahel PF. Locking plates: tips and tricks. *J Bone Joint Surg Am* 2007;89:2298–307. doi:10.1097/00005131-200409000-00003.
- [19] Bengard MJ, Gardner MJ. Screw depth sounding in proximal humerus fractures to avoid iatrogenic intra-articular penetration. *J Orthop Trauma* 2011;25:630–3. doi:10.1097/Bot.0b013e318206eb65.
- [20] Jin L, Guo JJ, Guo JJ, Yin Y, Hou Z, Zhang Y. Clinical effects of the probing method with depth gauge for determining the screw depth of locking proximal humeral plate. *Biomed Res Int* 2016;2016:5898161. doi:10.1155/2016/5898161.

- [21] van Rooyen RS, Marsh A, Strick NE, Hong T, Meeghan CO. Humeral head collapse causing locked screw penetration of the glenohumeral joint. *Inj Extra* 2006;37:462–5. doi:10.1016/j.injury.2006.06.024.
- [22] Poitout D.G. Biomechanics and biomaterials in orthopedics, second edition. 2016. doi:10.1007/978-1-84882-664-9.
- [23] Kowalski RJ, Ferrara LA, Benzel EC. Biomechanics of the spine. *Neurosurg Q* 2005;15:42–59. doi:10.1097/01.wnq.0000152406.39871.8e.
- [24] Bai L, Fu ZG, An S, Zhang PX, Zhang DY, Jiang BG. Effect of calcar screw use in surgical neck fractures of the proximal humerus with unstable medial support: a biomechanical study. *J Orthop Trauma* 2014;28:452–7.
- [25] Gardner MJ, Weil Y, Barker JU, Kelly BT, Helfet DL, Lorch DG. The importance of medial support in locked plating of proximal humerus fractures. *J Orthop Trauma* 2007;21:185–91. doi:10.1097/Bot.0b013e3180333094.
- [26] Osterhoff G, Baumgartner D, Favre P, Wanner GA, Gerber H, Simmen HP, et al. Medial support by fibula bone graft in angular stable plate fixation of proximal humeral fractures: an in vitro study with synthetic bone. *J Shoulder Elb Surg* 2011;20:740–6. doi:10.1016/j.jse.2010.10.040.
- [27] Lin S-J, Tsai Y-H, Yang T-Y, Shen S-H, Huang K-C, Lee MS. Medial calcar support and radiographic outcomes of plate fixation for proximal humeral fractures. *Biomed Res Int* 2015;2015:1–8. doi:10.1155/2015/170283.
- [28] Zhang L, Zheng JY, Wang WL, Lin GM, Huang YJ, Zheng J, et al. The clinical benefit of medial support screws in locking plating of proximal humerus fractures: a prospective randomized study. *Int Orthop* 2011;35:1655–61. doi:10.1007/s00264-011-1227-5.
- [29] Frich LH, Jensen NC. Bone properties of the humeral head and resistance to screw cutout. *Int J Shoulder Surg* 2014;8:21–6. doi:10.4103/0973-6042.131851.
- [30] Namdari S, Lipman AJ, Ricchetti ET, Tjoumakaris FP, Russell Huffman G, Mehta S. Fixation strategies to prevent screw cut-out and malreduction in proximal humeral fracture fixation. *Clin Orthop Surg* 2012;4:321–4. doi:10.4055/cios.2012.4.4.321.
- [31] Badman BL, Mighell M. Fixed-angle locked plating of two-, three-, and four-part proximal humerus fractures. *J Am Acad Orthop Surg* 2008;16:294–302.
- [32] Schumer RA, Muckley KL, Markert RJ, Prayson MJ, Heflin J, Konstantakos EK, et al. Biomechanical comparison of a proximal humeral locking plate using two methods of head fixation. *J Shoulder Elb Surg* 2010;19:495–501. doi:10.1016/j.jse.2009.11.003.
- [33] Yamamoto N, Hongo M, Berglund LJ, Sperling JW, Cofield RH, An KN, et al. Biomechanical analysis of a novel locking plate with smooth pegs versus a conventional locking plate with threaded screws for proximal humerus fractures. *J Shoulder Elb Surg* 2013;22:445–50. doi:10.1016/j.jse.2012.04.005.
- [34] Mehling I, Klitscher D, Mehling AP, Nowak TE, Sternstein W, Rommens PM, et al. Volar fixed-angle plating of distal radius fractures: screws versus pegs—a biomechanical study in a cadaveric model. *J Orthop Trauma* 2012;26:395–401. doi:10.1097/BOT.0b013e318225ea46.
- [35] Weninger P, Dall'Ara E, Leixnering M, Pezzeri C, Hertz H, Drobetz H, et al. Volar fixed-angle plating of extra-articular distal radius fractures—a biomechanical analysis comparing threaded screws and smooth pegs. *J Trauma Inj Infect Crit Care* 2010;69:E46–55. doi:10.1097/TA.0b013e3181c6630e.
- [36] Martineau PA, Waitayawinyu T, Malone KJ, Hanel DP, Trumble TE. Volar plating of AO C3 distal radius fractures: biomechanical evaluation of locking screw and locking smooth peg configurations. *J Hand Surg Am* 2008;33:827–34. doi:10.1016/j.jhsa.2008.01.006.
- [37] Yao J, Park MJ, Patel CS. Biomechanical comparison of volar locked plate constructs using smooth and threaded locking pegs. *Orthopedics* 2014;37:e169–73. doi:10.3928/01477447-20140124-21.
- [38] Boretto JG, Pacher N, Giunta D, Gallucci GL, Alfie V, De Carli P. Comparative clinical study of locking screws versus smooth locking pegs in volar plating of distal radius fractures. *J Hand Surg Eur Vol* 2014;39:755–60. doi:10.1177/1753193413517806.
- [39] Inzana JA, Varga P, Windolf M. Implicit modeling of screw threads for efficient finite element analysis of complex bone-implant systems. *J Biomech* 2016. doi:10.1016/j.jbiomech.2016.04.021.
- [40] Kennedy J, Feerick E, McGarry P, FitzPatrick D, Mullett H. Effect of calcium triphosphate cement on proximal humeral fracture osteosynthesis: a finite element analysis. *J Orthop Surg (Hong Kong)* 2013;21:167–72.
- [41] He Y, He J, Wang F, Zhou D, Wang Y, Wang B, et al. Application of additional medial plate in treatment of proximal humeral fractures with unstable medial column: a finite element study and clinical practice. *Medicine (Baltimore)* 2015;94:e1775. doi:10.1097/MD.0000000000001775.
- [42] Aalco Metals Ltd.. Stainless steel - grade 316 datasheet 2013;3–5. <http://www.azom.com/article.aspx?ArticleID=863>.
- [43] Sawbones. Biomechanical Test Materials. 2017.
- [44] Biomet-Trauma. S3 humerus plating system - surgical technique 2014.
- [45] Jabran A, Peach C, Zou Z, Ren L. Hybrid blade and locking plate fixation for proximal humerus fractures: a comparative biomechanical analysis. *Biomed Eng Online* 2018;17. doi:10.1186/s12938-018-0447-y.
- [46] Karunratanakul K, Schrooten J, Van Oosterwyck H. Finite element modelling of a unilateral fixator for bone reconstruction: Importance of contact settings. *Med Eng Phys* 2010;32:461–7. doi:10.1016/j.medengphy.2010.03.005.
- [47] MacLeod AR, Pankaj P, Simpson AHRW. Does screw-bone interface modelling matter in finite element analyses? *J Biomech* 2012;45:1712–16. doi:10.1016/j.jbiomech.2012.04.008.
- [48] Yang P, Zhang Y, Liu J, Xiao J, Ma LM, Zhu CR. Biomechanical effect of medial cortical support and medial screw support on locking plate fixation in proximal humeral fractures with a medial gap: a finite element analysis. *Acta Orthop Traumatol Turc* 2015;49:203–9. doi:10.3944/AOTT.2015.14.0204.